Optical Materials 31 (2009) 1488–1491

Contents lists available at ScienceDirect

Optical Materials

journal homepage: www.elsevier.com/locate/optmat

Polymeric waveguides using oxidized porous silicon cladding for optical amplification

D. Navarro-Urrios [a,*], M. Ghulinyan [b], P. Bettotti [a], E. Rigo [a], C.J. Oton [c], N.E. Capuj [d], F. Lahoz [e], I.R. Martín [e], L. Pavesi [a]

[a] Nanoscience Laboratory, Department of Physics, University of Trento, via Sommarive 14, I-38100 Povo (Trento), Italy
[b] Advanced Photonics and Photovoltaics, FBK-IRST, via Sommarive 18, 38100 Povo (Trento), Italy
[c] Optoelectronics Research Centre, University of Southampton, Highfield, Southampton SO17 1BJ, United Kingdom
[d] Dpto. de Física Básica, University of La Laguna, Tenerife, Spain
[e] Dpto. de Física Fund. y Exp. Electr. y Sist., University of La Laguna, Tenerife, Spain

ARTICLE INFO

Article history:
Received 6 August 2008
Received in revised form 2 February 2009
Accepted 15 February 2009
Available online 18 March 2009

PACS:
42.79.G
42.70.J
61.43.G

Keywords:
Optical amplification
Silicon
Polymers
Gain
Laser dye

ABSTRACT

We report on a new hybrid approach to realize optical slab waveguides for optical amplification purposes. The structure consists of a dye-doped polymer core (PMMA) deposited over an oxidized porous silicon (PS) cladding layer formed on a silicon wafer. The very low refractive index ($n = 1.16$) achievable in the cladding allows obtaining monomodal behavior with high confinement factors ($\Gamma_{TE} = 96\%$) even for very thin cores (400 nm). Optically excited guided luminescence shows stimulated emission, strong line narrowing and a clear threshold and superlinear behavior with pump energy. By means of the variable stripe length (VSL) technique, values of net optical gain up to 113 dB/cm (constant over 3 mm) and absolute amplification values up to 34 dB have been measured at 694 nm when pumping with 80 mJ/cm^2 energy pulses. These results validate the use of oxidized PS as a cladding layer in silicon photonics.

1. Introduction

Polymers are very attractive for the fabrication of active and passive optical components [1–3] because they have a good combination of low cost production, flexibility and toughness [4]. In addition, they can be easily patterned using ultraviolet and electron beam writing, hot embossing techniques, or spin-coated onto pre-patterned substrates. Many encouraging results on optical amplification and even laser action have been reported in polymer based devices, where the active material is a laser dye dissolved within the polymer (see for example Refs. [5,6]), rare earth ions to have infrared amplification [7] or even the polymer itself [8]. For those reasons it is of high interest to combine their optical properties with those of silicon, thus adding to the attributes of the latter coherent light emission, one of the major challenges in silicon photonics.

One of the main drawbacks of many polymers used in optical applications is that they have refractive indices which are not easily compatible with the requirements of silicon photonics. The large refractive index of silicon (3.5) and silicon oxide (1.45) make both materials frequently unsuitable for coupling with a polymer layer. Indeed, there are many polymers with refractive indices between 1.5 and 1.3 which are too similar to that of silica. As a consequence, optical components fabricated on silicon have to be formed by a multilayer polymeric structure with a few percent index contrast between the cladding and the core layer, which in turn means large footprint if high modal confinement factors are wanted. In this work we demonstrate a system which allows tight integration of polymer based active optical components on silicon.

Our approach to overcome these limitations is to use a porous silica glass cladding material obtained by strong oxidation of porous silicon (PS). Oxidation converts PS into a porous SiO_2 glass, with a tailored low material refractive index (from 1.16 to 1.45) and negligible absorption of visible light [9]. These two characteristics make this material very appealing for waveguiding applications in the visible range. It is worth noting that our approach is very similar

* Corresponding author.
E-mail address: dnavarro@el.ub.es (D. Navarro-Urrios).

0925-3467/$ - see front matter © 2009 Elsevier B.V. All rights reserved.
doi:10.1016/j.optmat.2009.02.008

to that of holey fibres, in which the core is solid and the cladding region is peppered with many small air holes that run the entire fibre length and lower the effective refractive index of the cladding.

The most common technique for the formation of PS is electrochemically etching of a silicon substrate [10], where it is possible to control the material refractive index with the etching current density. This raises the possibility of growing high quality vertical 1D photonic structures [11], PS and oxidized PS optical waveguides [12,13], where the refractive index of the top layer is higher than that of the bottom.

Due to its low cost and its transparency in the visible range, polymethylmethacrylate (PMMA) is a promising material in hybrid organic–inorganic optical components. In this work, we combine the properties of PMMA with that of porous silica to form organic/inorganic hybrid waveguides. Indeed, we demonstrate the presence of optical gain and, additionally, we validate the use of porous silica as an extremely low refractive index material with good optical qualities to be used in compact optical devices for silicon photonics.

2. Experimental details

Porous silicon samples were fabricated by electrochemical etching of heavily doped (0.01 Ωcm resistivity) p-type silicon. Single monolayer samples were grown by applying a constant current density of 80 mA/cm^2 on a 1 cm^2 circular surface. The refractive index of oxidized PS can be varied from 1.16 to 1.45 by modifying the etching currents and annealing treatment. In the studied samples, the annealing treatment was done at 900 °C for 3 h in order to completely oxidize the structures, turning them into porous silica with a refractive index of 1.16, the lowest refractive index which is possible to achieve. More details on the oxidized PS formation and characterisation of our samples are reported elsewhere [9,12]. The AFM images were recorded in tapping mode (AFM tip: NT-MDT NSG01, curvature radius typical 6 nm, guaranteed 10 nm, recording speed 1 Hz, in plane step around 8 nm). Roughness analysis was performed after image planarization obtained by subtracting 2nd order polynomial curve, line-by-line. The roughness definition we used is the "Root Mean Square" defined as

$$S_q = \sqrt{\frac{1}{MN}\sum_{r=0}^{M-1}\sum_{s=0}^{N-1}[z(x_r, y_s)]^2}.$$

Regarding the polymer core of the waveguides, a visible laser dye, Nile Blue (LC 6900) [14,15], was dissolved in the precursor PMMA solution at various molar concentrations (10^{-6}–10^{-3} M). The resulting solution was successively spin-coated onto the already grown cladding, where the core thickness was controlled by the spin-coater rotating speed, i.e. a higher velocity implies a greater centrifugal force, which allows depositing thinner layers. As a final step, the spin-coated films were baked for 10 min at 160 °C over a hot plate. The optimum dye concentration for our amplification purposes was determined to be 4×10^{-3} M, which is the one used in the discussed samples. It is also worth noting that in the present paper we report on the results for the most compact monomodal slab waveguide with the highest confinement factors, since we have used a cladding with the lowest refractive index achievable.

The properties of the modes supported by the slab waveguides were studied with a prism coupling (m-line) technique at 632.8 nm, schematized in the top part of Fig. 1. With this method, accurate characterisation of waveguide modes can be performed and the refractive index and thickness of the core and cladding layers can be extracted, since there is a straight relationship between the angle incidence on the prism and the effective refractive index

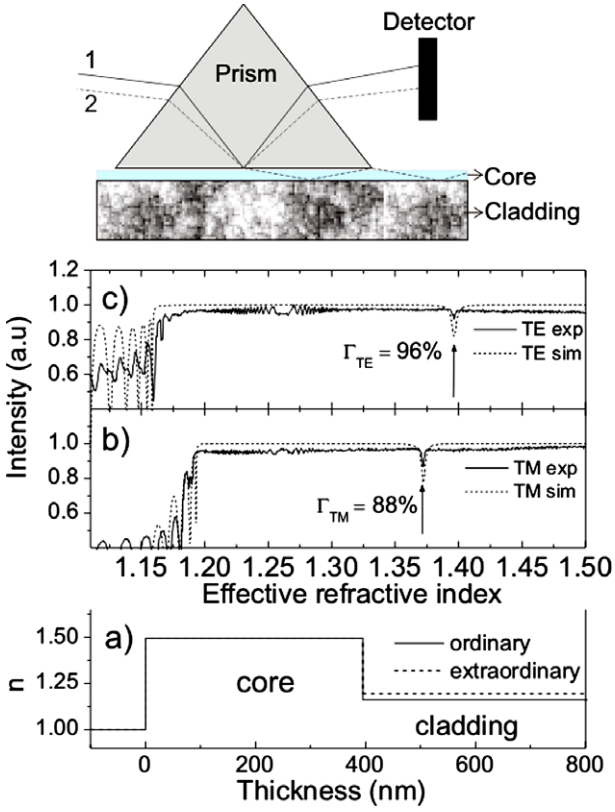

Fig. 1. M-line measurements (continuous line), simulations (dotted line) for TE (panel b) and TM (panel c) polarization. The arrows show the position of the dark line due to the propagating mode. Panel (a) refers to the refractive index profile for the ordinary (continuous line) and extraordinary (dotted line) rays extracted from the simulations.

of the propagating light. More details on this technique are reported elsewhere [16].

Amplification and losses measurements were performed by optically pumping the slab waveguides with the 532 nm line of a pulsed (5 ns) frequency doubled Nd-YAG laser operating in Q-switching mode. The pump laser with energy E_p was focused onto the slab waveguide surface in a stripe 1.5 cm long and 300 μm wide, by means of a cylindrical lens. A metal blade was placed in front of the waveguide, so that it was possible to vary the illumination length L with micrometric resolution by moving the blade edge. The guided emission spectra from the polymeric thin film were obtained by collecting the emission from the waveguide edge. Emission spectra have been analysed by a monochromator interfaced with a photomultiplier tube (PMT)

The optical losses of the waveguides were measured using the shifting excitation spot (SES) technique, which consists in scanning a pump spot over the waveguide surface and measuring the guided luminescence versus the distance d of the pump spot from the edge [17]. Gain measurements were performed by means of the variable strip length (VSL) technique [18]. In the VSL technique, the sample is optically excited by a narrow pumping stripe. The length L of the stripe can be varied by displacing the position of the metal blade. It is worth noting that we have taken all of the precautions described in [19] to avoid possible experimental artefacts. An amplified spontaneous emission (ASE) signal I_{ASE} was therefore collected from the edge of the waveguide, which increases as a function of L according to:

$$I_{ASE}(L) \propto \frac{1}{g}(e^{gL} - 1) \quad (1)$$

where g is the pump energy dependent gain coefficient. In our experiment, one single laser shot was used for each L value.

3. Results and discussion

Fig. 1 shows the results of the m-line measurements and simulations for both TE and TM polarizations together with the extracted refractive index profiles. The presence of only one dark line (pointed by the arrows) in the m-line measurements indicates that the waveguide is monomodal. We have simulated the experimental data by using software that applies the transfer matrix method and calculates the angular dependence of the reflectivity of a multilayer stack of dielectric materials. The refractive indices and thicknesses of core and cladding are taken as the free parameters of the model. This leads to the material refractive index profile represented in the bottom panel of Fig. 1, which is the one that best reproduces the m-line experimental result. The simulated curves of reflectance vs effective refractive index (related with incident angle) using this refractive index profile are represented with dashed lines in Fig. 1. As a result, we have extracted the different waveguide parameters, which are:

(1) Refractive index of the core n_{core} ~1.49;
(2) Core thickness d_{core} ~0.395 μm;
(3) Refractive index and thickness of the cladding n_{clad} ~1.16 and d_{clad} ~5 μm, respectively;
(4) Material birefringence $B = 3\%$ of the cladding layer, due to the vertical structure of the pores [20,21];
(5) Optical confinement factor for the TE mode $\Gamma_{TE} = 96\%$ and for the TM mode $\Gamma_{TM} = 88\%$.

Changes as small as 1% in the values of refractive indices and thickness reported on the previous list reflect in a perceptible shifting of the absorption line from the measured position, which is therefore the precision of our procedure.

It is worth noting that if a waveguide with the same core is grown over bulk silica, the thickness needed to start guiding (with a confinement factor less than 24%) is at least 500 nm, and more than 1 μm is needed to achieve similar Γ to that for a porous silica cladding.

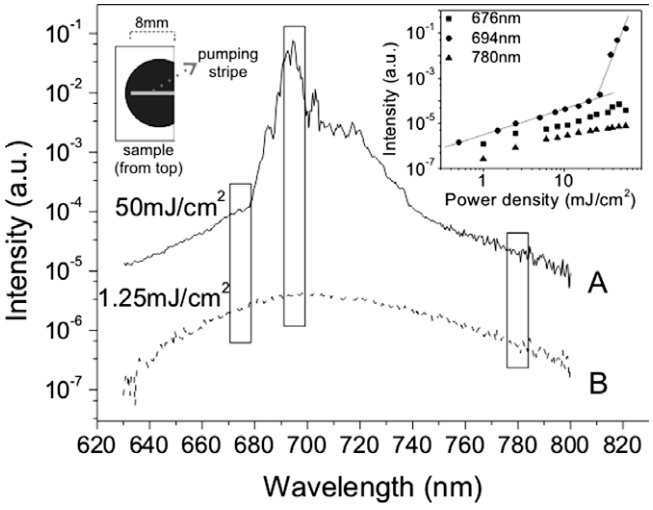

Fig. 2. Guided emission spectra for high (A, solid line) and low (B, dashed line) pump energy when pumping with a stripe ~8 mm long (the experimental conditions are shown in the top left part of the figure). The right inset shows the integrated emission intensities for three different 5 nm wide portions of the emission spectra around the indicated wavelengths versus pump energies.

Having already presented the information regarding the effective refractive indices and confinement factors of the supported modes, hereafter we report on the passive (optical losses) and active (optical amplification) properties of those modes when they propagate through the waveguides. In Fig. 2 we show the guided emission spectra due to emission from the pump excited dye molecules, for high and low pump energy (in logarithmic scale). At low energy the spectrum is a single wide band, while at high energy a narrow and fine-structured emission band emerges from a wide emission background. The inset shows the integrated emission intensity versus pump energy density of a few 5 nm wide portions of the emission band, centred at 676, 694 and 780 nm, respectively. Linear behaviors are observed for both 676 and 780 nm slices while a threshold at about 30 mJ/cm^2 and a subsequent highly superlinear increase (the slope of the curve is much higher than 1) is observed for the 694 nm slice. This is a first evidence of stimulated emission above the threshold.

Losses measurements using the SES technique have been performed. In Fig. 3 we show the curves obtained for 694 and 780 nm. From an exponential decay fit, it is possible to extract the propagation losses of guided light in the slab waveguides in cm^{-1} (number on the curves in Fig. 3). At 676 nm the measurement allowed extracting only a lower limit to the loss coefficient, which is about 65 cm^{-1} due to the dye absorption. We have checked the influence of the modal confinement on the losses by changing the refractive index of the cladding and we found that the higher refractive index of the cladding (the lower confinement) the lower the loss coefficient. This behavior is opposite to what would be expected if the source of the losses were the core-cladding interfaces, because less confinement significantly increases the interaction of the optical mode with the interface roughness [22]. We have performed atomic force microscopy (AFM) measurements on the surface of the oxidized PS substrate (Fig. 4) and found that roughness to be less than 4 nm, which means that losses due to interface roughness between core and cladding are negligible. Thus, we claim that the main source of the propagation losses is direct absorption by the dye within the core and that the cladding is of very high optical quality. However, quite high losses values (15 cm^{-1}) were found also at 780 nm, where the dye in the solution did not have appreciable absorption [14]. This effect could be associated with absorption of dye agglomerates (accumulation of dye molecules that did not dissolve well within the original polymeric solution) within the core or perhaps to scattering due to inclusions in the core, such as voids, cracks or bubbles, present when doping the polymer with the laser dye molecules. In any case

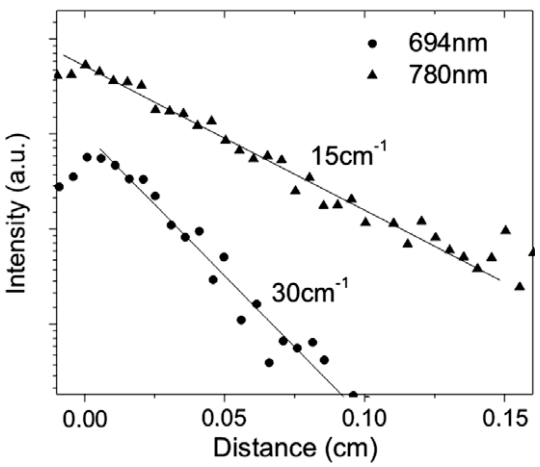

Fig. 3. Shifting excitation spot curves for different wavelengths, 694 (●) and 780 nm (▲) with exponential decay fits (lines). The labels on the curves refer to the loss coefficients.

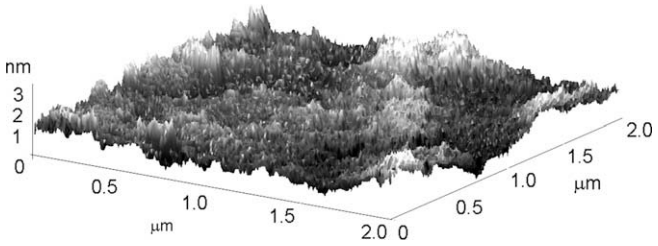

Fig. 4. Atomic force microscopy measurement of one of the oxidized porous silicon layers used as a cladding layer.

the strong relation between the losses and the presence of the dye is demonstrated by the low losses (4 cm^{-1} at 730 nm) measured in a slab waveguide with an order of magnitude lower dye concentration (not shown).

Panel (a) of Fig. 5 shows the variable stripe length (VSL) measurements performed for different pump energy densities recording the ASE at 694 nm. For low pump energy (E_p), a sublinear behavior of $I_{ASE}(L)$ is observed. By fitting the data with Eq (1), a loss coefficient equal to that measured by SES is found. When E_P increases above threshold, $I_{ASE}(L)$ becomes a positive exponential. Note the four orders of magnitude of increase in ASE over a few mm. This is the second evidence of positive optical gain in our slab waveguides. The maximum obtained gain coefficient was of 26 cm^{-1}, which corresponds to 113 dB/cm. An absolute amplification value of 34 dB is achieved by pumping 3 mm of the sample at 80 mJ/cm^2. For pumping lengths greater than 3 mm the overall gain gets saturated since the generated ASE signal is so high that modifies the excited level population so strongly that the stimulated processes dominate the dynamics of the system. At this point stimulated emission and absorption compensate and the material becomes transparent.

In the panels (b) and (c) of Fig. 5 we show the emission spectra obtained when illuminating with different pumping lengths L, for high (panel b) and low (panel c) pump energies. At low pump energy, no major effects are observed when L is increased from 1 to 8 mm and even red-shift due to self-absorption is not appreciable because of the high losses. At high pump energy, a narrow fine-structured band at 700 nm emerges when L is increased. Note that in this experiment the pump density is kept constant. This behavior is a third evidence of ASE due to optical gain when the pump is increased over the threshold.

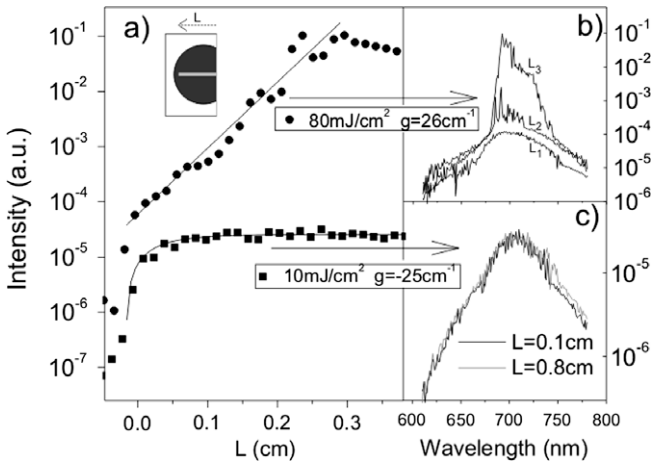

Fig. 5. (a) Variable stripe length measurements at 694 nm for low (■) and high (●) pump energy. The results of the fits to Eq. (1) are shown in the legends. Intensities are comparable. Guided emission measured pumping with different excitation lengths (L_1 = 0.02 cm, L_2 = 0.05 cm and L_3 = 0.25 cm) at high pump energy (panel b) and at low pump energy (panel c).

Laser dyes in a solid matrix are easier to handle than when in liquids. However, photostability is a big issue in solid-state dye-doped gain media. Actually, the high pump intensity causes a degradation of the dye molecule. In a way comparable to that observed in similar samples with oxidized PS core, this effect resulted in a displacement of the pump energy threshold towards higher values [12].

Finally, we want to stress that, although within this work we have not done a fully optimisation of the active core, we have obtained high values of net optical gain in the visible, comparable to that reported in literature for much more improved active materials (see for example Ref. [6]).

4. Conclusions

We have demonstrated slab optical waveguides using a new approach, in which the cladding layer is made of very low refractive index porous silica and the core layer is made of PMMA doped with a laser dye. Evidence of a large net optical gain at 694 nm has been reported in several different ways, which could open new routes towards realizing low cost – high performance optical amplifiers or lasers. We believe that the amplification properties (pump power threshold and passive losses) of these particular waveguides under study will be much improved when a systematic work on the optimisation of the active polymeric core will be done. Therefore, we emphasize that the use of oxidized PS as cladding layer would allow the deposition of low refractive index polymers on silicon to form compact optical devices.

Acknowledgements

We acknowledge FBK-irst Trento for the spin-coating procedure. This work has been supported by Ministerio de Educación y Ciencia (MAT2004-6868) and Gobierno Autónomo de Canarias (PI042004/018).

References

[1] N. Tessler, G.J. Denton, R.H. Friend, Nature London 382 (1996) 695.
[2] F. Hide, M.A. Diaz-Garcia, B. Schwartz, M. Andersson, G. Pei, A.J. Heeger, Science 273 (1996) 1833.
[3] S. Frovlov, W. Gellerman, M. Ozaki, K. Yoshino, Z.V. Vardeny, Phys. Rev. Lett. 78 (1996) 729.
[4] Hong Ma, Alex K.-Y. Jen, Larry R. Dalton, Adv. Mater. 14 (2002) 1339.
[5] G. Jordan, M. Flämmich, M. Rüther, T. Kobayashi, W.J. Blau, Y. Suzuki, T. Kainom, Appl. Phys. Lett. 88 (2006) 161114.
[6] K. Yamashita, T. Kuro, K. Oe, H. Yanagi, Appl. Phys. Lett. 88 (2006) 241110.
[7] A.Q. Le Quang, R. Hierle, J. Zyss, I. Ledoux, G. Cusmai, R. Costa, A. Barberis, S. Pietralunga, Appl. Phys. Lett. 89 (2006) 141124.
[8] A.E. Vasdekis, S.A. Moore, A. Ruseckas, T.F. Krauss, I.D.W. Samuel, G.A. Turnbull, Appl. Phys. Lett. 91 (2007) 051124.
[9] D. Navarro-Urrios, Ph. D. Thesis, University of La Laguna, 2006.
[10] O. Bisi, S. Ossicini, L. Pavesi, Surf. Sci. Rep. 264 (2000) 1–126.
[11] M. Ghulinyan, C.J. Oton, G. Bonetti, Z. Gaburro, L. Pavesi, J. Appl. Phys. 93 (2003) 9724.
[12] C.J. Oton, D. Navarro-Urrios, N.E. Capuj, M. Ghulinyan, L. Pavesi, S. González-Pérez, F. Lahoz, I.R. Martín, Appl. Phys. Lett. 89 (2006) 011107.
[13] P. Pirasteh, J. Charrier, Y. Dumeige, P. Joubert, S. Haesaert, A. Chaillou, L. Haji, P. Le Rendu, T.P. Nguyen, Phys. Status Solidi A 202 (2005) 1712.
[14] U. Brackmann, Lambdachrome Laser Dyes, third ed., Lambda Physik®, Germany, 2000.
[15] D. Navarro-Urrios, M. Ghulinyan, P. Bettotti, N. Capuj, C.J. Oton, F. Lahoz, I.R. Martin, L. Pavesi, Proc. SPIE 6593 (2007) 659321.
[16] P.K. Tien, R. Ulrich, R.J. Martin, Appl. Phys. Lett. 14 (1969) 291.
[17] J. Valenta, I. Pelant, J. Linnros, Appl. Phys. Lett. 81 (2002) 1396.
[18] K.L. Shaklee, R.E. Nahaori, L.F. Leheny, J. Lumin. 7 (1973) 284.
[19] L. Dal Negro, P. Bettotti, M. Cazzanelli, D. Pacifici, L. Pavesi, Opt. Commun. 229 (2004) 337.
[20] D. Kovalev, G. Polisski, J. Diener, H. Heckler, N. Künzner, V. Yu, F. Timoshenko, F. Koch, Appl. Phys. Lett. 78 (2001) 91.
[21] C.J. Oton, Z. Gaburro, M. Ghulinyan, L. Pancheri, P. Bettotti, L. Dal Negro, L. Pavesi, Appl. Phys. Lett. 81 (2002) 4919.
[22] K.K. Lee, D.R. Lim, H.-C. Luan, A. Agarwal, J. Foresi, L.C. Kimerling, Appl. Phys. Lett. 77 (2000) 1617.